

High-Resolution Transmission Electron Microscopy of Crystal Transformation in Solution-Grown Lamellae of Isotactic Polybutene-1

Masatoshi Tosaka,* Takashi Kamijo,† Masaki Tsuji, Shinzo Kohjiya, Tetsuya Ogawa, Seiji Isoda, and Takashi Kobayashi

Division of States and Structures, Institute for Chemical Research, Kyoto University, Uji, Kyoto-fu 611-0011, Japan

Received August 28, 2000

ABSTRACT: The crystal transformation in lamellar crystals of polybutene-1 grown from an amyl acetate solution was studied by cryogenic high-resolution transmission electron microscopy. The shape of the transformed trigonal (form-1) crystal domains in the surrounding tetragonal (form-2) crystal was successfully revealed. Along with the nucleation of the “untwinned” form-1, the existence of another nucleation mechanism which creates the “twinned” form-1 was suspected. Each crystallite of form-1 was comparatively large, and accordingly, the growth of the form-1 crystal was thought to progress not stem by stem but by pulling in the molecular chains from the surrounding form-2, creating new stems of form-1. Once form-1 has nucleated, mutual orientation between the form-1 and the form-2 domains appeared to be insignificant for further growth. The shape of the form-1 domain was irregular, and no specific crystallographic direction along which the form-1 domain tends to grow was found.

Introduction

Isotactic polybutene-1 (PB1) is a thermoplastic material of industrial interest in the field of water pipes as an substitute for poly(vinyl chloride), because PB1 has comparatively good chemical/heat resistance¹ and is free from the elution of endocrine disruptor. Three major crystalline forms have been reported for PB1 so far. Form-1 is characterized by the trigonal unit cell² (space group $R\bar{3}c$ or $R\bar{3}c$; $a = 1.77$ nm, c (chain axis) = 0.65 nm) and 3/1 helical conformation of backbone chains. Form-2 has the tetragonal unit cell³ ($P4$; $a = 1.542$ nm, c (chain axis) = 2.105 nm) in which four molecular chain stems with 11/3 helical conformation are packed. In form-3, molecular chains with 4/1 helical conformation are packed in the orthorhombic unit cell⁴ ($P2_12_12_1$; $a = 1.238$ nm, $b = 0.888$ nm, and c (chain axis) = 0.756 nm). The interconversion between various physical forms of PB1 is schematically shown in Figure 1. The samples as-polymerized with the Ziegler-type catalyst contain form-1 and form-3.⁵ Melt crystallization usually leads to the formation of form-2.^{3,6–14} However, when PB1 is melt-crystallized under high hydrostatic pressure ($> ca.$ 1000 atm),^{15,16} by a special melt-stretching technique¹⁰ or onto specific substrates for epitaxial growth,^{17,18} formation of form-1 has been reported. Formation of form-3 has also been reported when PB1 is melt-crystallized with a specific nucleating agent.^{4,17} In the case of crystallization from a dilute amyl acetate solution, all three forms can be obtained by controlling dissolution and crystallization temperatures.^{19,20} When form-1 and form-3 were formed directly from the melt or from the amyl acetate solution, they transform into form-2 by annealing at 90–100 °C (probably through a melting–recrystallization process).^{15,20} It is interesting that form-2 gradually transforms into form-1 on aging at room temperature.^{7–13,19–21} In the case of solution-

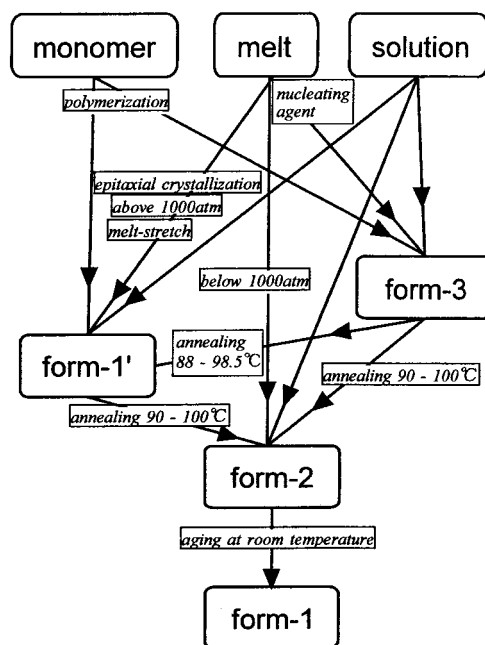


Figure 1. Interconversion between various physical forms of PB1. For simplicity, only an amyl acetate solution is considered in this figure.

grown single crystals, morphological change induced by this transformation is not observed except for formation of small cracks.²⁰ The form-1 specimen that was obtained by transformation from form-2 is the most stable and does not change into form-2 even when the sample is annealed again.²⁰ In this context, form-1 that is formed directly and can transform into form-2 by annealing is denoted as form-1'. Because form-1' showed broader crystalline reflection peaks in the X-ray spectrum than form-1, form-1' has been regarded to be an imperfect form-1 with many defects.⁵

It is still unclear, in terms of the molecular movements, how form-2 transforms into form-1 without changing the original shape.²⁰ In the early work by

* Corresponding author. Telephone: +81-774-38-3063. Fax: +81-774-38-3069. E-mail: tosaka@scl.kyoto-u.ac.jp.

† Present address: Core Technology Center, Nitto Denko Corp., 1-1-2, Shimohozumi, Ibaraki, Osaka-fu 567-8680, Japan.

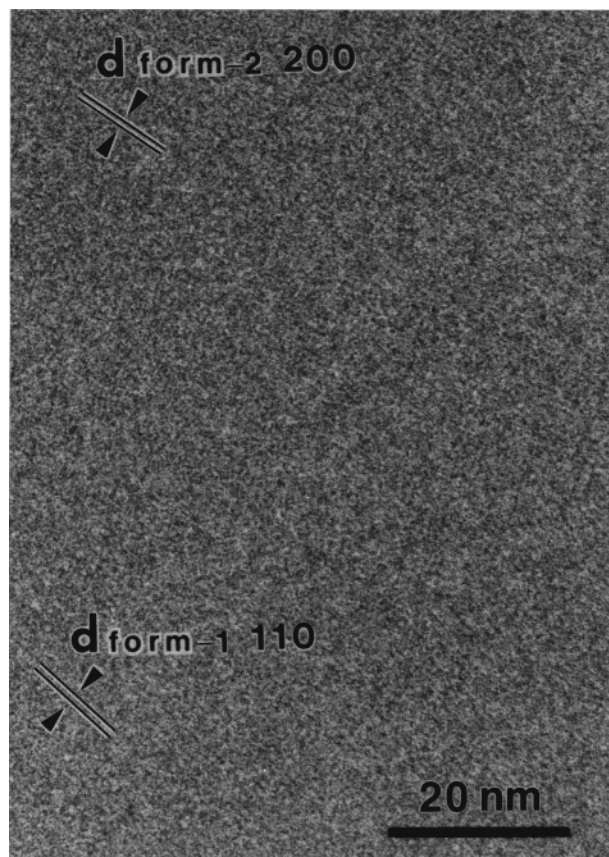


Figure 2. High-resolution image of PB1 single crystal before processing, which was taken at 4.2 K. The preparation conditions of the specimen were as follows: $T_s = 140\text{ }^{\circ}\text{C}$, $T_c = 80\text{ }^{\circ}\text{C}$, and $t_c = 2\text{ h}$. The specimen was kept at room temperature for 1 day before taking the TEM photograph.

Holland and Miller,²⁰ the formation of form-1 crystals twinning along the diagonals of the original square-shaped single crystal of form-2 was proposed; it was assumed that each quadrant of the square is an “untwinned” form-1 and adjacent quadrants are rotated by 90° with respect to each other. However, the twinning may not be essential for the transformation. Fujiwara¹¹ investigated the transformation of oriented form-2 specimens and found that the “untwinned” form-1 appears by applying shear stress; the orientation of form-1 changed according to the relative direction of the stress. He proposed a nucleation mechanism for the transformation. Kopp et al.²¹ investigated the form-2 single crystals grown from an octanol solution by transmission electron microscopy (TEM), and their observation was explained by the molecular mechanism proposed by Fujiwara. For example, in the dark-field (DF) image of the transformed form-1 crystal, many “cracks” running parallel to the (110) plane that is common for form-1 and form-2 were found. The “cracks” were thought to accommodate the shrinkage of the transformed crystal which is expected by expanding Fujiwara’s nucleation model.^{21,22} However, such “cracks” in DF images were not recognized in the bright-field (BF) images of the same area (in our experiment; an example will be shown in the later part of this article), and accordingly, the interpretation about the “cracks” is not satisfactory.

For further discussion, information concerning to the transformation at molecular level is desired. In this paper, solution-grown lamellar crystals of PB1 are

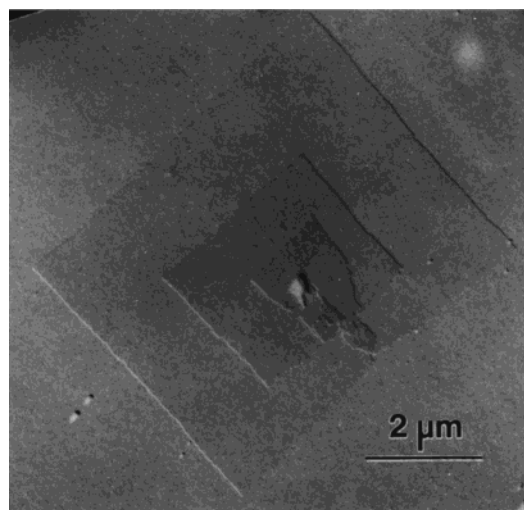


Figure 3. Morphology of the form-2 single crystal. The specimen ($T_s = 140\text{ }^{\circ}\text{C}$, $T_c = 70\text{ }^{\circ}\text{C}$, $t_c = 1\text{ h}$) was shadowed with Pt-Pd.

studied by high-resolution transmission electron microscopy (HREM). To overcome the problem of the electron irradiation damage, a cryogenic transmission electron microscope^{23–26} which can cool the specimen down to liquid helium temperature (4.2 K) was utilized along with the built-in minimum dose system (MDS).²⁷ The shape of each crystal domain is discussed on the basis of the distribution of corresponding lattice fringes in the HREM image.

Experimental Section

The PB1 sample (TW85305; $M_n = 1.86 \times 10^5$, $M_w = 9.17 \times 10^5$ on the basis of polystyrene standard) was kindly supplied by Sumitomo Chemical Co., Ltd. The as-received sample was dissolved in amyl acetate to be an 0.01 or 0.02 wt % solution. Isothermal crystallization was performed by putting a test tube containing the solution into an oil bath thermostated at the prefixed crystallization temperature (T_c). It is known that the dissolution temperature (T_s) is important in controlling the crystal form to be obtained.²⁰ In this study, T_s is selected from the temperatures between 120 and $140\text{ }^{\circ}\text{C}$. The preparation conditions including T_s , T_c , and crystallization time (t_c) will be described where appropriate. Single crystals suspended in the solution were taken out with a pipet and deposited on a copper grid for TEM on which an evaporated carbon support film had been put. Additional treatments such as metal shadowing were applied as the need arises.

Morphological observations and selected-area electron diffraction (ED) experiments were performed using a conventional transmission electron microscope (JEOL JEM-200CS) operated at 160 or 200 kV. For high-resolution observations, a cryogenic transmission electron microscope (JEOL JEM-4000SFX; 400 kV) was used. In this case, the built-in MDS was utilized and the specimen was cooled to the liquid helium temperature (4.2 K) to suppress electron irradiation damage. Before taking the high-resolution image, the total end-point dose (TEPD)^{25,26} of PB1 crystal was measured from the electron current density on the fluorescent screen and from the time length at which the crystalline reflections totally disappear; $(\text{TEPD value}) = (\text{magnification on the screen})^2 \times (\text{current density}) \times (\text{time length})$. At room temperature, the TEPD value of the PB1 crystal for 200 kV electron beams had been measured to be $100\text{ electrons}\cdot\text{nm}^{-2}$ (ca. $16\text{ C}\cdot\text{m}^{-2}$).^{25,26} On the other hand, the TEPD value at 4.2 K for 400 kV electron beams was increased up to ca. $390\text{ C}\cdot\text{m}^{-2}$, showing the effectiveness of cryoprotection.^{23–26} On the basis of this TEPD value, the electron dose to take one micrograph was set to be $140\text{ C}\cdot\text{m}^{-2}$ at a direct magnification of 5×10^4 . In practice, the micrographs were taken at a dose between 130 and $160\text{ C}\cdot\text{m}^{-2}$.

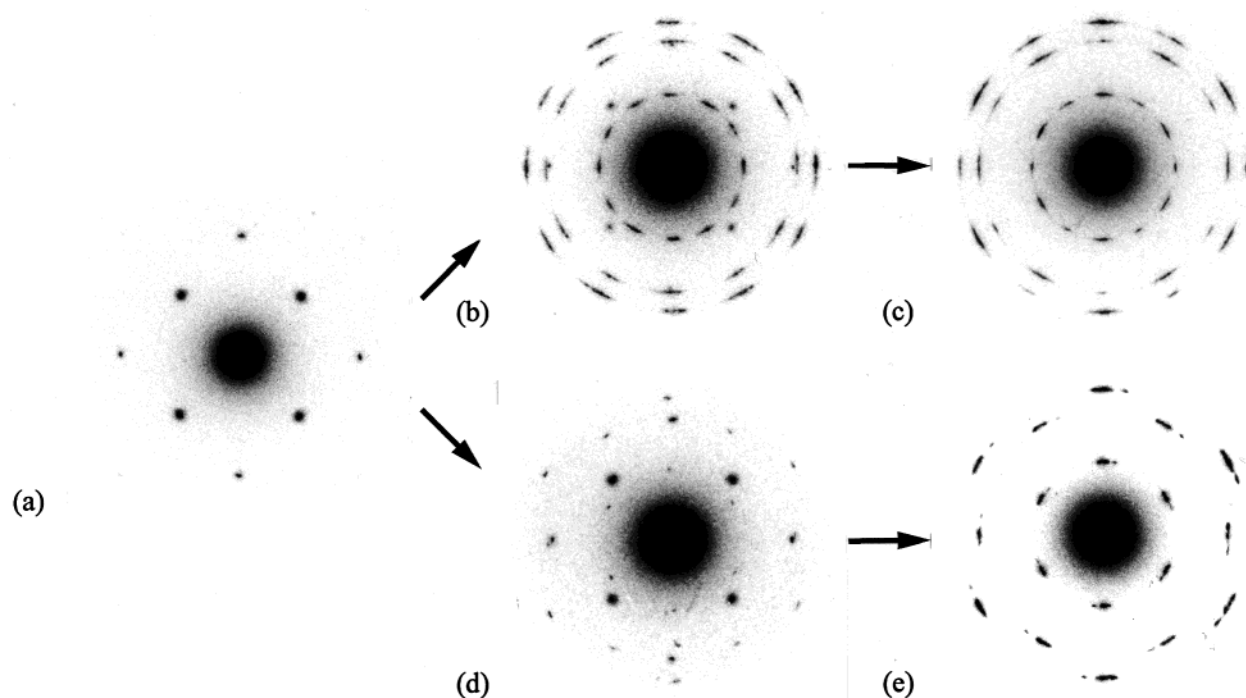


Figure 4. ED patterns from the square lamellar crystals kept for various days at room temperature: (a) just after crystallization ($T_s = 120\text{ }^{\circ}\text{C}$, $T_c = 60\text{ }^{\circ}\text{C}$, $t_c = 53\text{ h}$), (b) 5 days after crystallization ($T_s = 130\text{ }^{\circ}\text{C}$, $T_c = 60\text{ }^{\circ}\text{C}$, $t_c = 39\text{ h}$), (c) 7 days after crystallization ($T_s = 120\text{ }^{\circ}\text{C}$, $T_c = 60\text{ }^{\circ}\text{C}$, $t_c = 53\text{ h}$), (d) 5 days after crystallization ($T_s = 130\text{ }^{\circ}\text{C}$, $T_c = 60\text{ }^{\circ}\text{C}$, $t_c = 39\text{ h}$), and (e) 21 days after crystallization ($T_s = 120\text{ }^{\circ}\text{C}$, $T_c = 70\text{ }^{\circ}\text{C}$, $t_c = 22\text{ h}$).

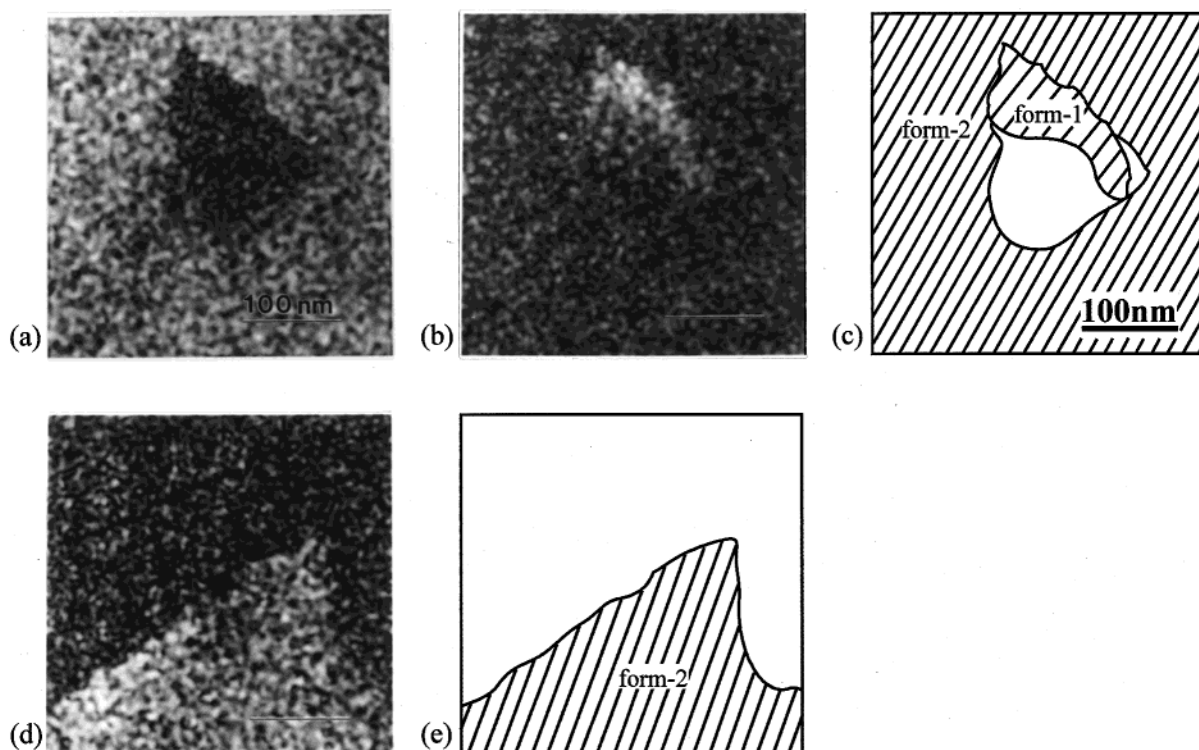


Figure 5. Partly transformed PB1 lamellar crystal. The preparation conditions of the specimen were as follows: $T_s = 120\text{ }^{\circ}\text{C}$, $T_c = 75\text{ }^{\circ}\text{C}$, and $t_c = 24\text{ h}$. The specimen was kept at room temperature for 4 days before taking the high-resolution TEM photograph. The bright regions are (a) form-2 and (b) form-1. The corresponding area and the orientation are summarized in part c, in which the stripes are drawn parallel to the (110) plane. The bright region in part d indicates another form-2 domain, and the area and the orientation are summarized in part e.

(In taking HREM images using MDS which enables focusing at a location slightly apart from the region to be photographed, exposure conditions including illumination and focusing are not accurately determined.) The ED patterns and the TEM images were recorded onto Mitsubishi MEM films, which were developed in full-strength Gekkol developer (Mitsubishi Paper

Mills Ltd.) at $20\text{ }^{\circ}\text{C}$ for 5 (ED and morphological work) or 10 min (high-resolution work).

Figure 2 shows an example of the high-resolution image of a lamellar crystal of PB1. In this figure, both the (110) fringes of form-1 and the (200) fringes of form-2 are recorded. The regions where these lattice fringes are located are regarded

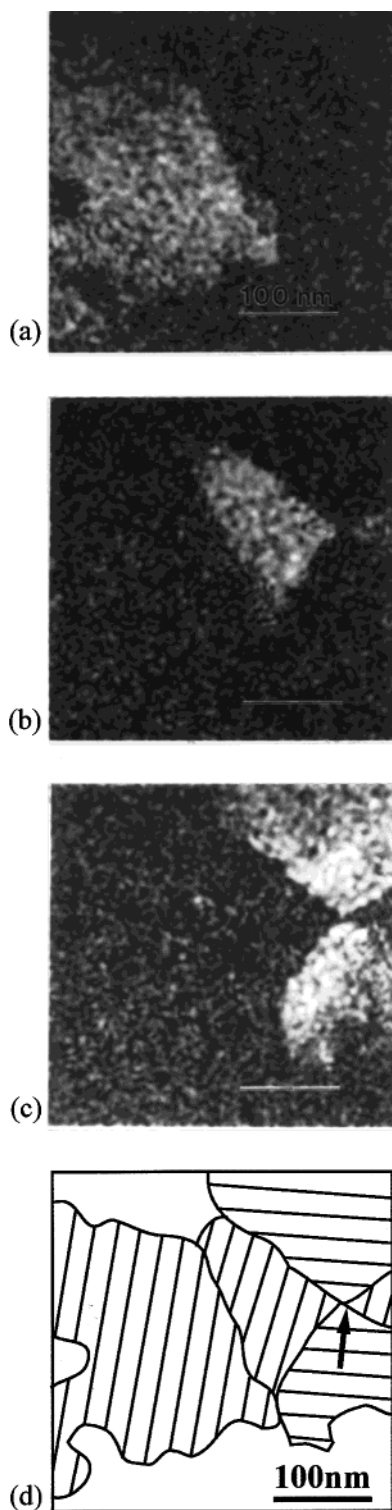


Figure 6. Transformed form-1 crystallites in a lamella. The preparation conditions of the specimen were as follows: $T_s = 120\text{ }^{\circ}\text{C}$, $T_c = 75\text{ }^{\circ}\text{C}$, and $t_c = 24\text{ h}$. The specimen was kept at room temperature for 4 days before taking the high-resolution TEM photograph. Each bright region in parts a–c is form-1 having a specific orientation. The area and the orientation are summarized in part d. The arrow in part d indicates the suspected nucleation point.

to be the corresponding crystalline domains. However, the fringes are difficult to recognize because of the poor signal-to-noise ratio. The high-resolution images were, therefore, processed with a computer for detection of the domains in which certain lattice fringes appear.²⁸ For this purpose, each high-resolution image recorded in the film was enlarged by

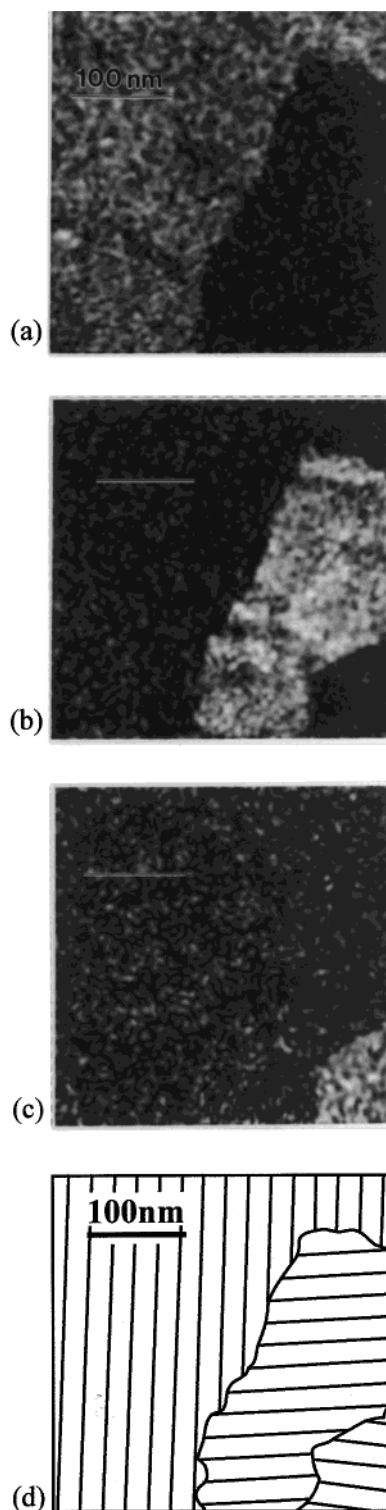


Figure 7. Transformed form-1 crystallites in a lamella. The preparation conditions of the specimen were as follows; $T_s = 130\text{ }^{\circ}\text{C}$, $T_c = 80\text{ }^{\circ}\text{C}$, $t_c = 100\text{ min}$. The specimen was kept at room temperature for 14 days before taking the high-resolution TEM photograph. Each bright region in parts a–c is form-1 having a specific orientation. The area and the orientation are summarized in part d. Note that the form-1 domains are in contact with each other and no vacancies are recognized.

printing off onto photographic paper and then the magnified photograph was scanned with an image scanner (SHARP JX-330X or EPSON GT9000) at an appropriate resolution. The digitized image data were transferred into a personal computer and a square region clipped from the data was processed, as mentioned below, with our homemade software written by an

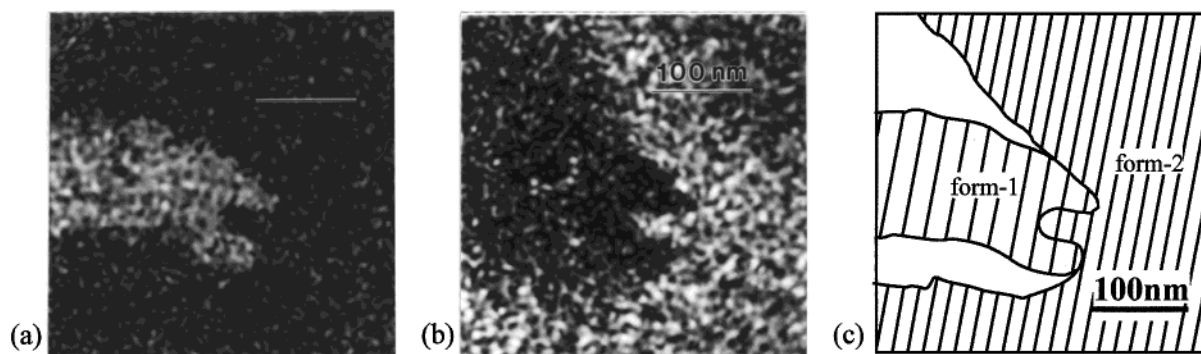


Figure 8. Partly transformed PB1 lamellar crystal. The preparation conditions of the specimen were as follows: $T_s = 120\text{ }^{\circ}\text{C}$, $T_c = 75\text{ }^{\circ}\text{C}$, and $t_c = 24\text{ h}$. The specimen was kept at room temperature for 4 days before taking the high-resolution TEM photograph. The bright regions are (a) form-2 and (b) form-1. The corresponding area and the orientation are summarized in part c. Note that the (110) plane of the form-1 domain is almost parallel to that of form-2.

image-processing language (Synoptics Semper6 for Windows). First, by applying a Fourier-filtering technique, an intermediate image was created from the original image using a pair of intensity maxima in the reciprocal space (viz., $hk0$ and $hk0$; the origin, 000, was not included in processing). This intermediate image showed the corresponding lattice fringes on the whole area; the strength (contrast) of the lattice fringes was different from place to place. The intermediate image was further processed by calculating the "local standard deviation" (LSD) of several (typically 5×5) pixels surrounding and including every given pixel. The LSD filter is a kind of smooth-edge detector and returns a larger value leading to an increase in brightness over a certain domain with inherent lattice fringes, namely lattice fringes that existed in the original image. By the image processing applied here, only the regions with inherent lattice fringes having a high contrast ought to be highlighted. The propriety of the image processing was made sure by comparing the processed image with the original one. We can also discuss the crystallographic orientation of the highlighted region by referring the Fourier transform (or the power spectrum) created as a step of this image processing.

Results and Discussion

Crystallization and Transformation. Holland and Miller²⁰ reported that only a small fraction (ca. 5%) of form-2 single crystals were grown from amyl acetate solution together with the majority of the form-3 crystals. However, as is written in their paper, the conditions for successful crystal growth (in this case, the growth of form-2) may be different from sample to sample. We, therefore, examined first the conditions that allow us to obtain a large enough amount of the form-2 single crystals from the amyl acetate solution. In the case of our PB1, most of the well-defined lamellar crystals grown at every T_c ranging from 60 to 100 $^{\circ}\text{C}$ for 1–24 h of crystallization time were in form-2. Figure 3 shows the typical morphology of the form-2 single crystal obtained in our experiment.

Figure 4 shows two series of ED patterns that indicate the occurrence of transformation. Just after the preparation, all the square crystals showed the ED pattern typical of form-2 (Figure 4a). After a few days of aging, reflections corresponding to form-1 appeared in the ED patterns from the square crystals (Figure 4b). After about an week, the reflections of form-2 disappeared and only those of form-1 were observed from most of the square crystals (Figure 4c). The transformed crystals usually showed the "twinned" hexagonal pattern.²⁰ This is essentially the same result as the in situ TEM observation of one lamellar crystal, which was reported by Holland and Miller.²⁰ We occasionally observed,

however, "untwinned" hexagonal patterns from the aged square crystals (parts d and e of Figure 4). A similar result, namely transformation into the "untwinned" form-1, has been reported by Kopp et al. for the single crystals prepared from an octanol solution.²¹

Nucleation of Form-1. Figure 5 shows a set of images processed from one of the high-resolution images. The bright regions in parts a and b of Figure 5 show the form-2 and form-1 domains, respectively. Since the small spots in the processed images should have come from the noise in the original micrograph, they were neglected. Figure 5c summarizes the arrangement of these form-2 and form-1 domains. The stripes in each domain are drawn as to be parallel to the (110) plane. (Hereafter, the stripes in this kind of illustrations are drawn parallel to the (110) plane.) Because there is only one form-1 domain of single orientation, form-1 seems to have nucleated in a manner which does not include twinning. Instead of the "twin" of form-1, we detected existence of another form-2 domain in this area, which is shown as the bright region in Figure 5d; the direction of the (110) lattice plane in this form-2 domain, namely the orientation of this domain, is slightly different from the one in Figure 5a. Obviously, this extra form-2 domain is attributed to another lamella (viz. a daughter lamella) piled on the one (viz. the mother lamella) shown in Figure 5, parts a–c, because one specific part of a lamellar crystal cannot have multiple crystal forms or orientations (the bright domain in Figure 5d is surely overlapping with the one in Figure 5a). Considering the fact that the lamellar crystal has been floating in the solution, the mother lamella should have suffered some stress at the edge of the daughter lamella; the edge of the daughter lamella could be a point of stress concentration for the mother lamella while the crystal was fluttering in the solution, or the mother lamella might be bent at the edge as it was deposited on the substrate and dried. It is proposed that the transformation is initiated by applying stress.^{10,12,21} In one case, the nucleation mechanism may be explained by, e.g., Fujiwara's theory,¹¹ namely, in a manner which does not involve the formation of twinned crystallites. Figure 5 may show such a location where the "untwinned" form-1 was nucleated.

Figure 6 shows another set of processed images. Each of the bright regions in Figure 6, parts a–c, shows the respective form-1 domains having a specific orientation. The arrangement of each form-1 domain is summarized in Figure 6d. The tothing of the five form-1 domains

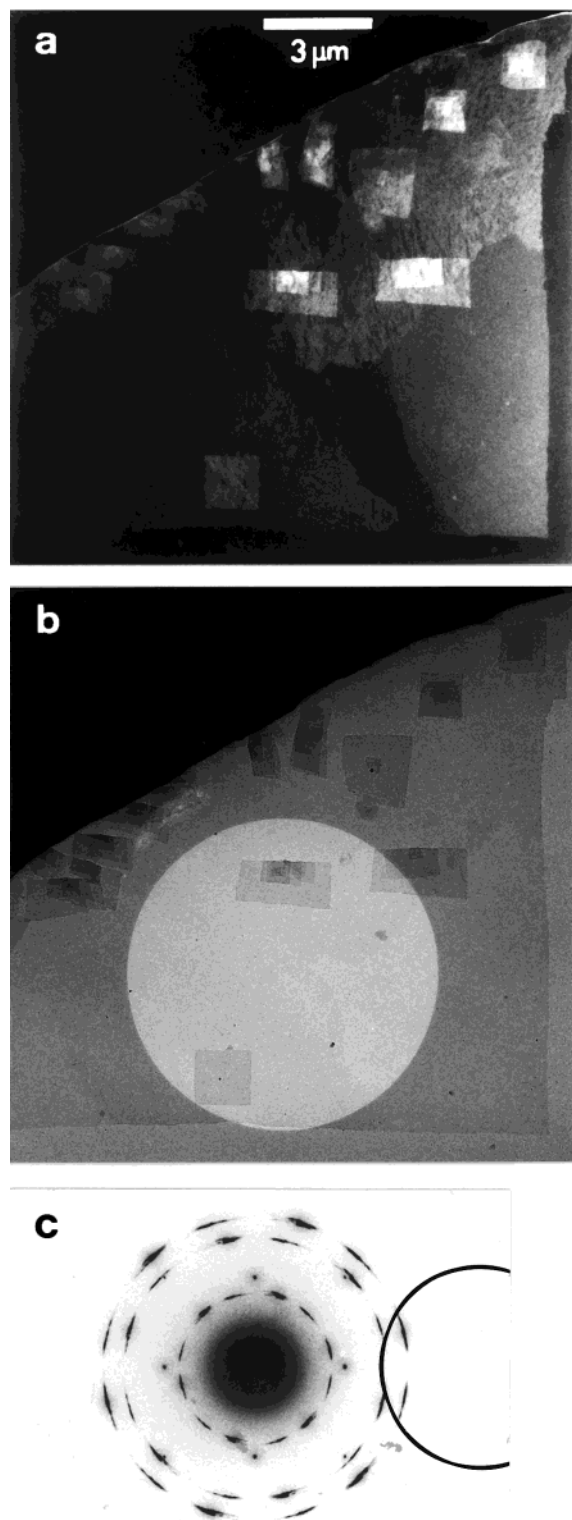


Figure 9. Partly transformed lamellar crystal of PB1. The preparation conditions of the specimen were as follows: $T_s = 140\text{ }^{\circ}\text{C}$, $T_c = 80\text{ }^{\circ}\text{C}$, and $t_c = 30\text{ h}$. The specimen was kept at room temperature for 26 days before TEM examination. (a) DF image taken using the 220 and other neighboring reflections of the "twinned" form-1. Because of the large size of the objective aperture equipped in our instrument, single 220 reflection could not be selected. (b) BF image taken in the diffraction mode of the microscope at large defocus of the same region. The circular bright region indicates the location of the selected-area aperture to take the ED pattern in part c. (c) ED pattern from the circular region in part b. Encircled reflections were used to take the DF image in part a.

without overlapping (like a jigsaw puzzle) indicates that only one lamellar crystal is involved in this region, in contrast to the case of Figure 5. It should be noted that four form-1 domains meet at one "point" (on a plane projected along the molecular chain) indicated by the arrow in Figure 6d. The convergence of separately nucleated four domains at one "point" should be statistically rare. Furthermore, each pair of the two domains opposed at the "point" has the same crystallographic orientation. Therefore, it is strongly believed that the four form-1 domains nucleated at the point indicated by the arrow as a twin crystal. It is interesting that the arrangement of these four form-1 domains is similar to the one proposed by Holland and Miller for the "twinned" form-1 crystals.²⁰ Fujiwara's theory¹¹ implicitly leads to nucleation on the stressed layer. On the other hand, Figure 6 suggests that there is another nucleating mechanism which is not caused by the stress but starts from a certain peculiar "point", creating the "twinned" form-1 crystallites.

Rearrangement of the Chain Molecules. Because of the conformational change, the transformation from form-2 to form-1 accompanies the increase in length (by ca. 13%) of a molecular stem which is composed of a given number of monomer units. At the same time, the density of the crystallites increases and the area for a given number of stems decreases (by ca. 24% on the *ab* plane). Accordingly, morphological changes such as lamellar thickening and formation of cracks in the lamella are expected as a result of the transformation.²¹

In the case of the bulk PB1 specimen, slight variations of the lamellar thickness and of the long period on the transformation have been reported by the use of small-angle X-ray scattering.²⁹ Holland and Miller also reported the formation of small cracks in the lamellae. However, in the TEM observation of PB1 single crystals, morphological changes on the transformation are not distinct, and we observed neither the variation of lamellar thickness nor the generation of the cracks in the BF images. (Even in our preliminary experiments by the use of an atomic force microscope which is much more sensitive to the height difference of the specimen, no morphological change was detected.)

A reasonable explanation for the virtually unchanged morphology may be that a considerable part of the increment of the stem length on the transformation is consumed to fill the vacancy which results from the density change. This explanation is based on a view that the form-1 domain grows by reeling in the molecular chains from the surrounding form-2 domain, uncoiling the form-2 crystallites and creating a new stem of form-1; the transformation may not progress stem by stem. We have reached to this view through our observation that each of the form-1 domains has a relatively large coherent area without vacancies. For example, Figure 7 shows a region where three crystallites of form-1 are closely packed without a discernible vacancy. If the transformation were to progress stem by stem without changing the number of stems, then some of the stems would have to travel several tens of nanometers of distance (much more larger than the stem length) to form such a large crystallite.

Progress of the Transformation. Once form-1 is nucleated, the orientational correlation between the form-1 and the form-2 domains, namely the relation $(110)_1 // (110)_2$, seems to be lost as the transformation progresses. This is known not only from the tangentially

arced reflections of form-1 in the ED pattern (Figure 4) but also from the processed high-resolution images. For example, in Figure 5c, the misalignment between the form-1 and the form-2 domains is ca. 9°, though the form-1 domain is relatively small. (Note that the maximum misalignment value is 15°, above which the other possible orientation of form-1 in the "twinned" relationship should be considered.) Furthermore, there may be no specific crystallographic direction along which the transformation propagates, because the transformed form-1 domain showed no specific crystallographic habits. Even when there is no orientational misalignment between the form-1 and the form-2 domains, the boundary is ill-shaped as if form-1 is "eating" the form-2 domain (Figure 8). On the basis of these observations, again, we propose that the form-1 domain is reeling in the molecular chains from the surrounding form-2 domain, and sometimes the traction force rotates the form-1 domain itself (probably at a very early stage of the transformation), leading to the orientational misalignment as is shown in Figure 5c.

DF observation of the partly transformed lamellar crystal, not the fully transformed one,²¹ was also successfully performed. Parts a and b of Figure 9 show the DF and the BF images, respectively, of the same region. The distribution of the form-1 region in Figure 9a indicates that the transformation takes place regardless of the growth sector of the original crystal, as has been pointed out by Kopp et al.²¹ It should be noted that, in our DF image (Figure 9a), "cracks" (dark striations) are running mostly in the direction parallel to one edge of the square crystal, namely, to the (100) plane of the original form-2 crystal. The "cracks" are not seen in the BF image, as is mentioned above. It seems that the direction of the "cracks" in the DF images is not related only to the molecular mechanism proposed by Fujiwara.¹¹

Concluding Remarks

When the transformation of PB1 from form-2 to form-1 is initiated by stress, the nucleation of form-1 may occur as was proposed by Fujiwara.¹¹ However, another type of nucleation mechanism which creates the "twinned" form-1 seems to exist. Once the form-1 domain is nucleated, it may grow by reeling in the molecular chains from the surrounding form-2 domains, creating new stems for form-1. The traction force to reel in the molecules may sometimes rotate the form-1 domain itself. After the nucleation, the form-1 domain may be able to grow even when there is misalignment in the relative orientation with the surrounding form-2 domain. There is no specific crystallographic direction along which the form-1 domain tends to grow, and accordingly, the shape of the form-1 domain is irregular.

Acknowledgment. Some of scanning works of the high-resolution images were performed by using the instruments in the Supercomputer Laboratory, Institute for Chemical Research, Kyoto University. This work was partly supported by the Society of Fiber Science and Technology, Japan, through the Young Scientist Award (to M. Tosaka, 1998), and also partly supported by a Grant-in-Aid for Scientific Research on Priority Areas, "Mechanism of Polymer Crystallization" (No. 12127207) from the Ministry of Education, Science, Sports, and Culture, Japan (to M. Tsuji, 2000—).

References and Notes

- (1) Luciani, L.; Seppälä J.; Löfgren, B. *Prog. Polym. Sci.* **1988**, *13*, 37.
- (2) Natta, G.; Corradini, P.; Bassi, I. W. *Nuovo Cimento, Suppl.* **1960**, *15*, 52.
- (3) Petraccone, V.; Pirozzi, B.; Frasci, A.; Corradini, P. *Eur. Polym. J.* **1976**, *12*, 323.
- (4) Dorset, D. L.; McCourt, M. P.; Kopp, S.; Wittmann, J. C.; Lotz, B. *Acta Crystallogr.* **1994**, *B50*, 201.
- (5) Boor, J., Jr.; Youngman, E. A. *J. Polym. Sci. B* **1964**, *2*, 903.
- (6) Turner-Jones, A. *J. Polym. Sci. B* **1963**, *1*, 455.
- (7) Boor, J., Jr.; Mitchell, J. C. *J. Polym. Sci.: Part A* **1963**, *1*, 59.
- (8) Powers, J.; Hoffman, J. D.; Weeks, J. J.; Quinn, F. A., Jr. *J. Res. Natl. Bur. Stand.* **1965**, *69A*, 335.
- (9) Schaffhauser, R. J. *J. Polym. Sci. B* **1967**, *5*, 839.
- (10) Gohil, R. M.; Miles, M. J.; Petermann, J. *J. Macromol. Sci.—Phys.* **1982**, *B21*, 189.
- (11) Fujiwara, Y. *Polym. Bull.* **1985**, *13*, 253.
- (12) Chau, K. W.; Yang, Y. C.; Geil, P. H. *J. Mater. Sci.* **1986**, *21*, 3002.
- (13) Hsu, T.-C.; Geil, P. H. *Polym. Commun.* **1990**, *31*, 105.
- (14) Tashiro, K.; Asanaga, H.; Ishino, K.; Tazaki, R.; Kobayashi, M. *J. Polym. Sci., Part B: Polym. Phys.* **1997**, *35*, 1677.
- (15) Armeniades, C. D.; Baer, E. *J. Macromol. Sci. Phys.* **1967**, *B1*, 309.
- (16) Nakafuku, C.; Miyaki, T. *Polymer* **1983**, *24*, 141.
- (17) Kopp, S.; Wittmann, J. C.; Lotz, B. *Polymer* **1994**, *35*, 908.
- (18) Kopp, S.; Wittmann, J. C.; Lotz, B. *Polymer* **1994**, *35*, 916.
- (19) Miller, R. L.; Holland, V. F. *J. Polym. Sci. B* **1964**, *2*, 519.
- (20) Holland, V. F.; Miller, R. L. *J. Appl. Phys.* **1964**, *35*, 3241.
- (21) Kopp, S.; Wittmann, J. C.; Lotz, B. *J. Mater. Sci.* **1994**, *29*, 6159.
- (22) Lotz, B.; Mathieu, C.; Thierry, A.; Lovinger, A. J.; De Rosa, C.; Ruiz de Ballesteros, O.; Auriemma, F. *Macromolecules* **1998**, *31*, 9253.
- (23) Tsuji, M.; Kohjiya, S. *Prog. Polym. Sci.* **1995**, *20*, 259.
- (24) Tsuji, M.; Tosaka, M.; Kawaguchi, A.; Katayama, K.; Iwatsuki, M. *Bull. Inst. Chem. Res., Kyoto Univ.* **1991**, *69*, 117.
- (25) Tosaka, M.; Tsuji, M.; Kohjiya, S. *Mater. Sci. Res. Int.* **1998**, *4*, 79.
- (26) Tosaka, M. In *Recent Research Developments in Macromolecules Research*; Pandalai, S. G., Ed; Research Signpost: Trivandrum, India, 1999; Vol. 4, Part I, p 45.
- (27) Fujiyoshi, Y.; Kobayashi, T.; Ishizuka, K.; Uyeda, N.; Ishida, Y.; Harada, Y. *Ultramicroscopy* **1980**, *5*, 459.
- (28) Tosaka, M.; Tsuji, M.; Cartier, L.; Lotz, B.; Kohjiya, S.; Ogawa, T.; Isoda, S.; Kobayashi, T. *Polymer* **1998**, *39*, 5273.
- (29) Marigo, A.; Marega, C.; Cecchin, G.; Collina, G.; Ferrara, G. *Eur. Polym. J.* **2000**, *36*, 131.

MA001495F